Journal of Thermal Analysis and Calorimetry, Vol. 89 (2007) 1, 267–275

REACTIONS OF DIVALENT TRANSITION METAL HALIDES WITH 3,5-DIMETHYL-1-(HYDROXYMETHYL)-PYRAZOLE
Part 23. Transition metal complexes with pyrazole-based ligands

V. M. Leovac[1], *R. Petković*[1], *A. Kovács*[2], *G. Pokol*[3] *and Katalin Mészáros Szécsényi*[1]*

[1]University of Novi Sad, Faculty of Sciences, Department of Chemistry, 21000 Novi Sad, Trg D. Obradovića 3 Serbia and Montenegro
[2]Hungarian Academy of Sciences, Budapest University of Technology and Economics, Research Group of Technical Analytical Chemistry, 1111 Budapest, Szt. Gellért tér 4, Hungary
[3]Institute for General and Analytical Chemistry, Budapest University of Technology and Economics, 1521 Budapest Szt. Gellért tér 4, Hungary

Factors determining the complex formation reaction of copper(II), nickel(II) and cobalt(II) chloride and copper(II) bromide with 3,5-dimethyl-1-(hydroxymethyl)-pyrazole (HL) has been studied. Depending on experimental conditions, complexes with different composition were obtained: $[CuCl_2(dmp)]_2$ (**I**), $[CuCl_2(dmp)_2]_2$ (**II**), $[CoCl_2(dmp)_2]$ (**III**) (*dmp*=3,5-dimethylpyrazole), $[CuBr(L)]_2$ (**IV**), $[CoCl(L)(EtOH)]_4$ (**V**) and $[NiCl(L)(EtOH)]_4$ (**VI**). The compounds were characterized by FTIR spectroscopy, solution conductivity and magnetic measurements. The crystal structure of $[CoCl(L)(EtOH)]_4$ has been determined by single crystal X-ray diffraction. The thermal decomposition of the compounds was studied and found to be continuous for all of the compounds. The desolvation mechanism of $[MCl(L)(EtOH)]_4$ (*M*=Co(II), Ni(II)) is explained on the basis of the route of complex formation of $CoCl_2$ with HL.

Keywords: *cobalt(II)-, copper(II)- and nickel(II) chloride and bromide complexes, 3,5-dimethyl-1-(hydroxymethyl)-pyrazole, 3,5-dimethylpyrazole, FTIR, TG, XRD*

Introduction

The resemblance of pyrazoles to imidazole derivatives as regular constituents of proteins makes the pyrazole based ligands as well as their complexes an attractive research area [1–5]. Complexes with pyrazole derivatives are often used to mimic enzymatic reactions which are very selective and conducted under mild conditions. Due to these characteristics of pyrazole complexes, there are attempts to test their catalytic activity to obtain specific industrial polymeric products [6]. One of their application fields includes thin film processing by metal organic chemical vapor deposition processes (MOCVD) [7–9] which claims for examining the thermal behavior of potential precursors including coupled TG-MS or TG-IR methods [10–16].

Our systematic studies on complexes with pyrazole based ligands aim to determine the key factors controlling the course of the complex formation [17–21]. The primary coordination site of pyrazole is its pyridine nitrogen atom, N(2). Depending on the nature and the position of the ring substituents, the number of coordination sites may be increased [22–24]. One of our main goals is to track the influence of various subsituents, changing them one by one. Besides, we are investigating how the structure of the compounds affects the course of their thermal decomposition. Special attention is paid to determine the structural characteristics of complexes whose thermal decomposition results in formation of relatively stable intermediates. The acquired knowledge of factors governing the course of the reaction and the thermal decomposition may serve to predict the experimental conditions for formation of compounds with a proposed composition.

In this paper we report the complex formation of copper(II), nickel(II) and cobalt(II) chloride and copper(II) bromide with 3,5-dimethyl-1-(hydroxymethyl)-pyrazole (HL) and selected physico-chemical properties of the formed compounds. As the 1-N-hydroxymethyl-group may be a subject of deprotonation, the role of base (KOH) in the course of the complex formation was also examined. The thermal decomposition of the compounds was determined by TG and DSC. From the obtained complexes $[CuCl_2(dmp)]_2$ (**I**), $[CuCl_2(dmp)_2]_2$ (**II**), $[CoCl_2(dmp)_2]$ (**III**) (*dmp*=3,5-dimethylpyrazole), $[CoCl(L)(EtOH)]_4$ (**V**) and $[NiCl(L)(EtOH)]_4$ **(VI)** [18, 25–27] are already known in the literature. The only novel complex obtained in the

* Author for correspondence: mszk@uns.ns.ac.yu

1388–6150/$20.00

Akadémiai Kiadó, Budapest, Hungary
Springer, Dordrecht, The Netherlands

present study is $[CuBr(L)]_2$ **(IV)**. However, the previous synthesis of the compounds was carried out under different conditions. Thus, reporting their synthesis gives contribution to understand the controlling factors of complex formation reactions. The thermal decomposition of **(I)**, **(II)** and **(III)** has also been reported [18] while for the other compounds it is determined here for the first time.

Experimental

Materials

Reagents

All chemicals were analytical grade commercially available products.

Syntheses

All the reactions were carried out with crystal hydrates of the corresponding metal salts in ethanolic solutions.

$[CuCl_2(dmp)]_2$, **I** (*dmp*=3,5-dimethylpyrazole): On mixing of solutions of $CuCl_2$ (2 mmol, in 13 cm^3 EtOH) and HL (0.24 g, 2 mmol, in 7 cm^3 EtOH) an immediate precipitation was observed. The yellow microcrystalline product **I**, was filtered off after 3 h, washed with cold ethanol and air dried. Yield: 52.0%. Found% (Calcd.%): C, 26.06 (26.04); H, 3.49 (3.56); N, 12.00 (12.15). FTIR spectrum (cm^{-1}, KBr): 3338s, 1571s, 1471m, 1413m, 1278s, 1184m, 1153m, 1049s, 1028m, 792m, 569m. λ_M=36.0 S cm^2 mol^{-1}.

$[CuCl_2(dmp)_2]_2$, **II**: 24 h after the precipitation of the mono(ligand) complex, **I**, green single crystals of **II** were obtained from the green colored filtrate. The crystals were washed with cold EtOH and dried on air. Yield: 6.1%. Found% (Calcd.%): C, 36.48 (36.76); H, 4.70 (4.94); N, 19.96 (17.15). FTIR spectrum (cm^{-1}, KBr): 3268s, 3203s, 3148m, 1571s, 1493m, 1472m, 1413m, 1275m, 1183m, 1171m, 1145m, 1050m, 1043m, 819m, 795m, 701m, 687m, 614m. λ_M=30.6 S cm^2 mol^{-1}.

$[CuBr(L)]_2$, **IV**: Solutions of 2 mmol of HL in 6 cm^3 EtOH with 10 drops of 10% KOH and 1 mmol $CuBr_2$ in 6 cm^3 of EtOH were mixed. Precipitation followed immediately which was dissolved in a boiling solution. The clean solution was left to cool to room temperature. The green precipitate was filtered off after 24 h, washed with cold EtOH and air dried. Yield: 52%. Found% (Calcd.%): C, 26.70 (26.83); H, 3.34 (3.38); N%: 10.10 (10.43). λ_M=39.4 S cm^2 mol^{-1}, μ_{eff}=1.66 μB. (The reaction of $CuBr_2$ with *L* has also been carried out without KOH. Mixing of 20 cm^3 solution containing 2 mmol $CuBr_2$ with 20 cm^3 solution of 2 mmol L, resulted in light green precipitate. It was filtered off after 24 h, washed with cold EtOH and dried at room temperature. Yield: 88.7%. Elemental analysis data, Found% (Calcd.%): C, 21.74 (20.62); H, 2.77 (2.88); N, 8.38 (8.02), λ_M=31.6 S cm^2 mol^{-1}, μ_{eff}=1.46 μ_B. In spite of the fact that the elemental analysis data and TG curves refer to a compound with a composition of $[CuBr_2(HL)]_2$ and the powder X-ray data suggest a different compound than that forming in the presence of KOH in a salt-to-ligand ratio of 1:2, the complex formation was not reproducible enough and a detailed discussion on this compound is omitted in this paper.)

$CoCl_2(dmp)_2$, **III**: In reactions of $CoCl_2 \cdot 6H_2O$ (1 mmol in 5 cm^3 EtOH) with HL (1 mmol in 2.5 cm^3 EtOH) in 1:1 and 1:2 mole ratio (2 mmol HL in 5 cm^3 EtOH) a blue 3,5-dimethylpyrazole complex, $CoCl_2(dmp)_2$, was obtained. The mixture was kept at room temperature for 5 h. The precipitate was filtered, washed with cold EtOH and air dried. The crystal structure of the compound is identical to that determined by Oki *et al.* [26]. Yield: about 20%. Found% (Calcd.%): C, 36.94 (37.29); H, 5.11 (5.01); N, 16.84 (17.39). λ_M=28.2 S cm^2 mol^{-1}.

$[CoCl(L)(EtOH)]_4$, **V**: The above described reaction was repeated in a salt-to-ligand mole ratio of 1:2 (1 mmol $CoCl_2 \cdot 6H_2O$ and 2 mmol of HL in EtOH, total volume of 10 cm^3) under reflux for 3 h. During a 12 h stay the same blue single crystals of **III** were formed, contaminated with crystals of **V** which were mechanically removed. The mother liquid was placed in a deep freezer. After 48 h deep purple single crystals of $[CoCl(L)(EtOH)]_4$ were obtained. The precipitate was filtered, washed with cold EtOH and air dried. The yield was about 10% calculated on the basis of $CoCl_2 \cdot 6H_2O$. When the reaction was carried out by mixing of cold (about 5°C) ethanolic solutions of the ligand and $CoCl_2$ and the mixture was kept in a deep freezer (at about –15°C) for 48 h, only the purple crystals of **V** were obtained, but the yield was even lower than in the former case. Found% (Calcd.%): C, 36.0 (36.18), H, 5.6 (5.69), N, 10.6 (10.55), λ_M=54.2 S cm^2 mol^{-1}.

$[NiCl(L)(EtOH)]_4$, **VI**: $NiCl_2 \cdot 6H_2O$ and HL were reacted in a salt-to-ligand mole ratio of 1:1 (1:1 mmol, total volume: 7.5 cm^3) and 1:2 (1:2 mmol, total volume: 10 cm^3) at room temperature. The reactions were carried out also in the presence of 5 drops (≈0.2 cm^3) of 10% KOH. In all the cases the same green single crystals of $[NiCl(L)(EtOH)]_4$ were formed, with a cubane-type structure determined previously by X-ray diffraction by Paap *et al.* [27]. Yield: about 25% in all four procedures. FTIR spectrum (cm^{-1}, KBr): 3414s, 2924m, 2887m, 1553vs, 1463s, 1423s, 1386s, 1257s, 1145m, 1101vs, 1051vs, 842s, 775s, 684s. Found% (Calcd.%): C, 34.78 (36.21); H, 5.41 (5.70); N, 10.29 (10.56). λ_M=69.5 S cm^2 mol^{-1}.

Methods

Elemental analysis (C,H,N) was performed by standard methods.

A single crystal of **V** with approximate dimensions of 0.08×0.08×0.12 mm^3 was selected for data collection.

The X-ray structure data were collected on a Bruker AXS SMART diffractometer with an APEX CCD detector, equipped with a Bede Microsource® X-ray generator, using MoK_α radiation. A full sphere of data was collected with a frame width of 0.3° and a counting time of 20 s per frame. A multiscan absorption correction [28] was applied to the raw data and the resulting R_{int} was 3.2%. Frames were integrated using the program SAINT [29]. The crystal structure was solved by direct methods using the SIR92 software [30] and refined using the Oxford Crystals suite [31]. The positions and atomic displacement parameters of all non-hydrogen atoms were refined; hydrogen atoms were located from difference Fourier maps and refined isotropically using restraints.

FTIR spectra were recorded at room temperature using KBr pellets in the range of 4000–450 cm^{-1} on a PerkinElmer System 2000 FTIR spectrometer with MCT detector and co-addition of 16 scans. The far-IR (650–150 cm^{-1}) measurements were carried out with polyethylene pellets and DTGS detector. The spectra were obtained with a resolution of 4 cm^{-1}.

Magnetic susceptibility measurements were conducted at room temperature on an MSB-MKI magnetic susceptibility balance Sherwood Scientific Ltd., Cambridge.

Molar conductivity of freshly prepared 10^{-3} mol dm^{-3} solutions in DMF was measured at room temperature using a digital conductivity meter Jenway 4010.

Thermal analysis was performed using a DuPont 1090 TA system with sample masses of about 5 mg. In the thermogravimetric measurements platinum crucible was employed, while the DSC curves were recorded up to 600 K using an open aluminum pan sample holder with an empty aluminum pan as reference. The measurements were carried out in both argon and air atmospheres at a heating rate of 10 K min^{-1}.

Results and discussion

In the reaction of HL with $CuCl_2$ the splitting of the 1-hydroxymethyl substituent occurs, leading to the formation of two *dmp* complexes, $[CuCl_2(dmp)]_2$ and $[CuCl_2(dmp)_2]_2$ (Scheme 1).

Barszcz *et al.* also investigated the complex formation reactions of copper(II) salts with HL [32, 33] depending on the solvent (mixtures of trimethyl orthoformate, methanol and propan-2-ol) used in the

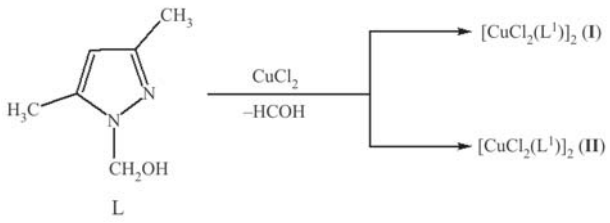

Scheme 1

preparation. With $Cu(NO_3)_2$ a mononuclear $[Cu(dmp)_3(NO_3)_2]$ was obtained, i.e., the same kind of splitting of the ligand was observed. In pure propan-2-ol Cu(II) salts gave binuclear complexes $[Cu(dmp)(L)X]_2$ (X=NO_3, BF_4, ClO_4), which means that only one ligand had lost HCOH, while the other ligand molecule coordinated in its deprotonated form. Splitting of the 1-N-substituent was also observed in the reaction of $CuCl_2$ with 1-carboxamide- 3,5-dimethylpyrazole, (L1, Scheme 2), [18]. The explanation of the phenomenon may partly be based on the HSAB principles [34–36] of binding preferences of the medium soft Cu(II) acid to the medium soft pyridine nitrogen (N_{py}) of the ring, taking into account the favorable steric effects caused by departing of the 1-N substituent. In reaction of copper(II) chloride with 1-(2-hydroxyethyl)-pyrazole (HL^1) in ethanolic solution no splitting of the 1-N-substituent was observed, instead, a spontaneous deprotonation of the ligand took place and $[Cu(L^1)X]_2$ was obtained [37]. Under similar experimental conditions with 3,5-dimethyl-1-thiocarboxamidepyrazole, (L2, Scheme 2) the ligand coordinated to the metal forming a neutral centrosymmetric $[Cu(L2)Cl_2]_2$ complex [38].

The mechanisms of reactions of $CuBr_2$ with L1 and L2 are different. In the reaction of $CuBr_2$ with 1-carboxamide-3,5-dimethylpyrazole (L1), one ligand molecule undergoes decarboxamidation [19] together with spontaneous deprotonation of the other ligand's carboxamide group. The binding preferences determined by the HSAB principle still hold in this molecule, but in addition, one voluminous bromide ion is replaced with the deprotonated ligand, via NH of the carboxamide group, reducing thus the steric repulsion

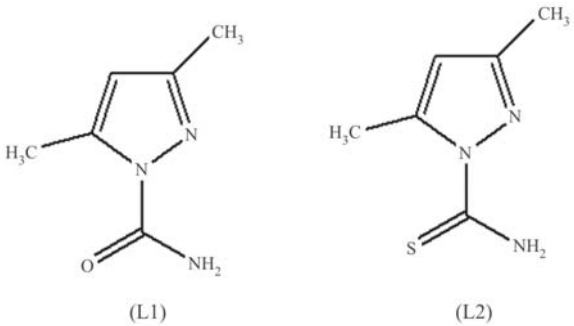

Scheme 2

inside the $[CuBr(dmp)(L1)]_2$ molecule. During the complex formation of $CuBr_2$ with 3,5-dimethyl-1-thiocarboxamide-pyrazole, (L2), Cu(II) is reduced to Cu(I), [38] leading to the same effect: the molecule contains only one bromide per copper(I) resulting in reduced steric repulsion in $[Cu_2Br_2(L2)_2]$. In addition, in the later complex the soft–soft interactions are dominant, except of that with the pyrazole N, which belongs to medium soft bases. In **IV**, with soft bromide bridges, the steric repulsions decrease, due to the deprotonation of CH_2OH-group in the presence of KOH. The binding preferences in the compound, according to the HSAB principles, between the medium soft Cu(II) acid, the medium soft pyrazole N and the somewhat harder deprotonated $–CH_2OH$ bases are still in the acceptable range, so neither the reduction of Cu(II) nor the splitting of N-substituent is taking place.

It is often found that the ligand anion formed by deprotonation replaces the counterion of the metal salt. Steric repulsions in such a molecule are usually reduced and, as a consequence, more stable compounds may form. In order to examine how the presence of a base affects the deprotonation of the ligand and the complex formation, the reactions with $CuBr_2$, $NiCl_2$ and $CoCl_2$ were carried out both with and without KOH.

In the reaction of $CuBr_2$ with 3,5-dimethyl-1-(hydroxymethyl)-pyrazole (HL) the deprotonation of the ligand occurs only when the $CuBr_2$ to HL ratio is 1:2. The salt-to-ligand ratio has no significant effect in reactions of $NiCl_2·6H_2O$ and $CoCl_2·6H_2O$ with HL. Our finding is that the reaction of $NiCl_2$ with HL is not affected by the presence or absence of the base: under all examined reaction conditions the only products are single crystals of **VI**, prepared by Paap *et al.* [26], in the presence of KOH. This means a spontaneous ligand deprotonation with nickel(II) chloride.

In the reaction of $CoCl_2$ with HL, in the presence of KOH, **III** was formed as the main product, i.e., the 1-N-substituent of the ligand had split, as with $CuCl_2$. From the mother liquid **V** was formed at low temperature in a deep freezer. The quality of the crystals allowed the crystal structure determination. The crystal data are presented in Table 1, while selected bond lengths and angles are given in Table 2. The molecular diagram and the atom numbering scheme of **V** is presented in Fig. 1 while a view of its packing is shown in Fig. 2. In the crystal, the chlorine atoms are

Table 1 Crystal data of $[CoCl(L)(EtOH)]_4$

Chemical formula	$C_{32}H_{60}Cl_4Co_4N_8O_8$
Molecular mass/amu	1062.42
Crystal system	monoclinic
Space group	$P2_1/n$
a/Å	13.3604(13)
b/Å	17.6288(18)
c/Å	20.268(2)
α/°	90
β/°	107.704(2)
γ/°	90
V/Å^3	4547.7(8)
Z	4
T/K	120
Calculated density/g cm^{-3}	1.552
μ/mm^{-1}	1.722
Total number of reflections	53721
Number of unique reflections	13230
Number of observed reflections ($I>2\sigma$)	8310
Number of parameters refined	745
R_{int}/%	3.50
R/% for I>2σ	3.04
wR/% for all reflections	9.11

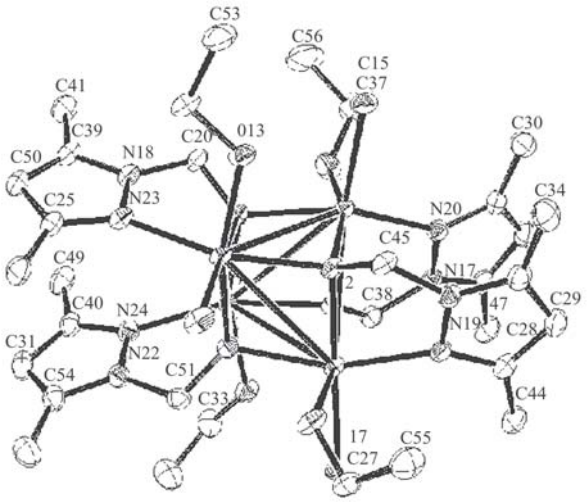

Fig. 1 The molecular diagram and the atom numbering scheme of $[CoCl(L)(EtOH)]_4$. Atomic displacement parameters are given at 50% probability level. Hydrogen atoms have been omitted for clarity

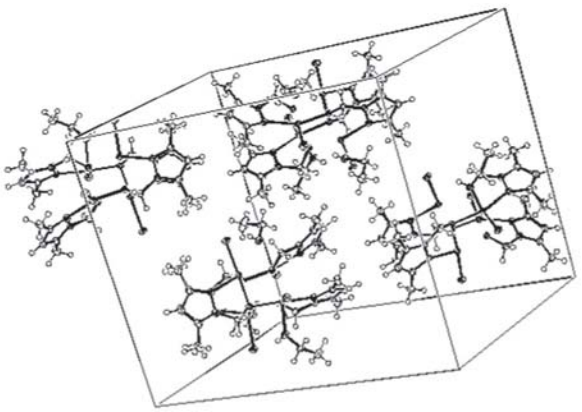

Fig. 2 Packing diagram for $[CoCl(L)(EtOH)]_4$

Table 2 Selected bond lengths (Å) and angles (°) of $[CoCl(L)(EtOH)]_4$

Length		Length	
Co(1)–Cl(5)	2.3722(8)	Co(1)–O(9)	2.0984(19)
Co(1)–O(16)	2.135(2)	Co(1)–N(20)	2.124(2)
Co(2)–O(11)	2.1177(18)	Co(2)–O(13)	2.142(2)
Co(3)–Cl(8)	2.3710(8)	Co(3)–O(9)	2.1369(18)
Co(3)–O(15)	2.1079(18)	Co(3)–N(24)	2.117(2)
Co(4)–O(11)	2.1118(18)	Co(4)–O(12)	2.1227(18)
O(9)–C(26)	1.400(3)	O(10)–C(27)	1.429(3)
O(13)–C(36)	1.442(3)	O(14)–C(33)	1.437(4)
N(17)–N(19)	1.369(3)	N(17)–C(42)	1.346(4)
N(18)–C(26)	1.467(4)	N(18)–C(39)	1.355(3)
N(20)–C(32)	1.343(4)	N(21)–C(38)	1.483(4)
N(22)–C(51)	1.474(3)	N(22)–C(54)	1.351(4)
Co(1)–O(11)	2.1414(18)	Co(1)–O(12)	2.1189(19)
Co(2)–Cl(6)	2.3676(8)	Co(2)–O(9)	2.1118(18)
Co(2)–O(15)	2.1464(19)	Co(2)–N(23)	2.120(2)
Co(3)–O(12)	2.1287(19)	Co(3)–O(14)	2.149(2)
Co(4)–Cl(7)	2.3761(8)	Co(4)–O(10)	2.108(2)
Co(4)–O(15)	2.1094(19)	Co(4)–N(19)	2.122(2)
O(11)–C(45)	1.385(3)	O(12)–C(38)	1.375(3)
O(15)–C(51)	1.381(3)	O(16)–C(37)	1.415(4)
N(17)–C(45)	1.478(3)	N(18)–N(23)	1.366(3)
N(19)–C(28)	1.339(3)	N(20)–N(21)	1.366(3)
N(21)–C(48)	1.351(4)	N(22)–N(24)	1.365(3)
N(23)–C(25)	1.331(4)	N(24)–C(40)	1.342(4)
Angle		Angle	
Cl(5)–Co(1)–O(9)	100.68(5)	Cl(5)–Co(1)–O(11)	92.80(5)
Cl(5)–Co(1)–O(16)	96.19(7)	Cl(5)–Co(1)–N(20)	102.93(7)
O(9)–Co(1)–O(12)	80.93(7)	O(9)–Co(1)–O(16)	84.99(8)
O(11)–Co(1)–O(12)	79.94(7)	O(11)–Co(1)–O(16)	163.42(8)
O(12)–Co(1)–O(16)	91.55(8)	O(12)–Co(1)–N(20)	77.04(8)
Cl(6)–Co(2)–O(9)	173.33(5)	Cl(6)–Co(2)–O(11)	99.23(5)
Cl(6)–Co(2)–O(15)	94.23(5)	Cl(6)–Co(2)–N(23)	104.09(6)
O(9)–Co(2)–O(13)	94.25(7)	O(9)–Co(2)–O(15)	79.11(7)
Cl(5)–Co(1)–O(12)	172.21(5)	O(16)–Co(1)–N(20)	82.70(9)
O(9)–Co(1)–O(11)	79.65(7)	Cl(6)–Co(2)–O(13)	92.29(6)
O(9)–Co(1)–N(20)	154.37(8)	O(9)–Co(2)–O(11)	79.89(7)
O(11)–Co(1)–N(20)	108.85(8)		

connected to the ethanolic OH groups by intramolecular hydrogen bonds.

The crystal structures of **II** and **III** have already been reported ([25, 26], respectively). However, we have checked their thermal decomposition in order to see how the route of the complex formation affects the decomposition pattern of the compounds. As the new copper(II) bromide complex, **IV**, could not be obtained in the form of single crystals, its composition and structure were proposed on the basis of elemental analysis data and FTIR spectroscopy. The band assignment is given in Table 3, together with a detailed IR-spectral analysis of **V** and **III**. The assignment was primarily based on quantum chemical computations on HL at the B3LYP/6-311++G** level and on *dmp* and $[CuBr(L)]_2$ at the B3LYP/6-31G** level using an effective core potential for Cu [39]. The spectral characterization of the other investigated

Table 3 Characteristic bands[a] in the FTIR spectra of $[CoCl(L)(EtOH)]_4$, $CoCl_2(dmp)_2$ and $[CuBr(L)]_2$

	$[CoCl(L)(EtOH)]_4$	$CoCl_2(dmp)_2$	$[CuBr(L)]_2$	Assignment[b]
1		3345s		ν_{N-H}
2		3313s		ν_{N-H}
3	2978m	2963w	2958m	$\nu_{as(CH_3)}$
4	2926m	2924m	2926m	$\nu_{as(CH_3)}$
5	2888m	2869vw	2882m	$\nu_{s(CH_3)}$
6	2879sh	2841vw	2868m	$\nu_{s(CH_3)}$
7	1552vs	1569vs	1548s	ν_{ring}
8	1479sh		1482m	sci CH_2
9	1463s	1470s	1462s	ν_{ring}, $\delta_{as(CH_3)}$
10	1422s	1406s	1420m	ν_{ring}, $\delta_{as(CH_3)}$
11	1386s	1378m	1389m	$\delta_{s(CH_3)}$
12	1378sh		1370s	wag CH_2
13	1260s	1271s	1245s	ν_{ring}, $\nu_{(N-CH_2)}$
14	1163m	1165s		δ_{ring}
15	1147m	1148s	1148s	δ_{ring}
16	1096vs	1099m	1089vs	ν_{C-O}, $\delta_{as(CH_3)}$
17	1047vs	1049vs	1057s	δ_{ring}
18	985m	983w	991sh	rock CH_3
19	839s		845m	$\nu_{(N-CH_2)}$
20	774s	819s	777m	wagC–H_{ring}
21	684s	703s	699s	τ_{ring}
22	629m	660m	626w	τ_{ring}
23	597vw	586m	571w	δ_{ring}
		427m		wagN–H

[a]The abbreviations vs, s, m, w, vw and sh mean very strong, strong, medium, weak, very weak and shoulder, respectively.
[b]Main components of the fundamentals. The symbols ν, δ and τ indicate stretching, deformation and torsion vibrations, respectively, while the abbreviations s, as, sci, wag and rock mean symmetric, asymmetric, scissoring, wagging and rocking, respectively

compounds is not given, only the characteristic bands are listed in the 'Experimental'.

The positions of the ν_{Co-Cl} bands in **III** at 340 and 308 cm^{-1}, as well as those of the ν_{Co-N} ones at 235 and 200 cm^{-1} are characteristic for tetrahedral coordination around Co(II) [40] in $CoCl_2(dmp)_2$, as was also found by single crystal structure determination [26].

For the novel $[CuBr(L)]_2$ complex the good agreement between the computed and experimental IR spectra supports the proposed structure presented in Scheme 3. The strong band in the far IR region at 398 cm^{-1} is assigned to ν_{Cu-O} on the basis of previous observations on related compound [33] supported also by the computations, while the ν_{Cu-N}, ν_{Cu-Br} and δ_{Cu-O} vibrations appear superimposed in a broad band in the 170–300 cm^{-1} region. The computations resulted in a distorted square-planar arrangement around the Cu atoms in the equilibrium structure of $[CuBr(L)]_2$ (cf. Scheme 3). The lower value of the magnetic moment relative to the spin-only value (μ_{eff}=1.66 μ_B) supports also the binuclear character of the complex [41]. Our search of the Cambridge Structure Database confirmed that the arrangement of ligands around Cu(II) for tetracoordinated complexes is generally distorted square planar (Scheme 3).

The molar conductivity data in DMF refer to the non-electrolyte character of all the compounds except the isomorphous cuban-type Ni(II), **VI**, and Co(II), **V**, complexes. The value of the molar conductivity of **VI** belongs to an electrolyte of 1:1 type, referring to a complete exchange of one chloride ion with DMF, while in **V** the conductivity is somewhat less than that corresponding to 1:1 electrolytes.

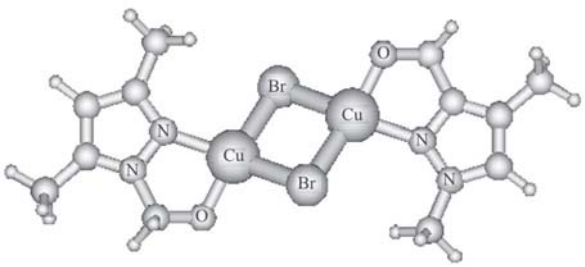

Scheme 3

Thermal decomposition of the compounds

The thermal decomposition of the reaction products of $CuCl_2$ with HL has been published recently [18]. Repeating the thermal analysis in the present study we obtained slightly different decomposition patterns due to the different structural characteristics, as a result of the different experimental conditions in the two studies. This is not an unknown phenomenon. The topology in chemistry refers to the so-called memory effect which means that compounds 'remember' the conditions under which they were produced [42]. In contrast to the decomposition of $[CuCl_2(dmp)]_2$ obtained with 1-carboxamide-3,5-dimethylpyrazole, where a relatively stable intermediate forms, the decomposition of the complexes obtained with 3,5-dimethyl-1-(hydroxymethyl)-pyrazole is continuous in the whole temperature range. The decomposition of $CoCl_2(dmp)_2$, **III**, with three clearly separated steps has a similar decomposition pattern as the corresponding copper(II) chloride complex, **II**, in spite of the fact that the later compound is a binuclear complex [25]. The thermal stability of **III** is higher by about 30 K (470 K). The composition of the end products of the decomposition in air (>800 K) was calculated on the basis of the mass losses. The percentage of the residue agree with pure metal end products (Co, found: 17%, calcd: 18.30%, Cu, found: 19%, calcd: 19.45%) and not $CoCl_2$ for **III**, as was found earlier [43]. (In our previous paper, [18], the percentage of the residue was even less, 17%. Unfortunately, the calculated value was given as CuO, but it was calculated for Cu. This means that the residue should be Cu, consistent with the findings presented in this paper. However, for an exact conclusion, the composition of the end products should be examined by powder X-ray analysis.) The decomposition of the *dmp* complexes in argon does not complete up to 1000 K.

The thermogravimetrical curves of the isomorphous cuban-type complexes, (**V** and **VI**) together with the TG curves of the bromide complex, **IV**, are presented in Fig. 3. All three compounds decompose without forming stable intermediates. Even the desolvated compounds could not be isolated.

The course of thermal decomposition of **V** and **VI** does not depend on the atmosphere and, except that in argon the decomposition is not completed up to 1000 K. The thermal stability of **VI** is higher by about 50 K (400 K) compared to **V**. As the compounds are isostructural, one would expect similar thermal decomposition patterns. They are, however, different. The desolvation of **VI** is a one-step process, loosing all four EtOH molecules in a temperature range of less than 80 K. In **V** the evaporation of the two most loosely bonded EtOH begins at 355 K and extends to about 70 K. At higher temperature the desolvation is accompanied with decomposition of the $[CoCl(L)]_4$ moiety. The IR-spectrum of an isolated degradation product of blue color at 580 K (about 20% mass loss) refers to the formation of **III**. However, the decomposition product is not stable (the decomposition of **III** begins at about 100 K lower temperature). The band assigned to ν_{ring} and ν_{N-CH_2} vibrations of **III** at 1271 cm^{-1} is present in the IR spectrum of the decomposition product, but with significantly lower relative intensity than found in the spectrum of **III**. Also the pyrrole ν_{N-H} vibrations of the *dmp* ligand show up at 3343 and 3340 cm^{-1}. The end products in air are most probably metal oxides (NiO, %, found: 29.0, calcd: 28.15; CoO, %, found: 27.0%, calcd: 28.21). The different desolvation mechanisms may originate from the preferences of the complex formation of $CoCl_2$ with HL: the main product of the reaction is **III**, while **V** is formed at low temperature in low yield, so the thermal decomposition probably goes through the formation of **III**, which is not stable at the decomposition temperature of **V**.

It can not be excluded that the different desolvation mechanism of the latter two compounds may be ascribed to the different distances between the central Ni(II) and Co(II) atoms and the coordinating oxygen atoms of EtOH molecules, presented in Table 4. However, to support this preposition one has to com-

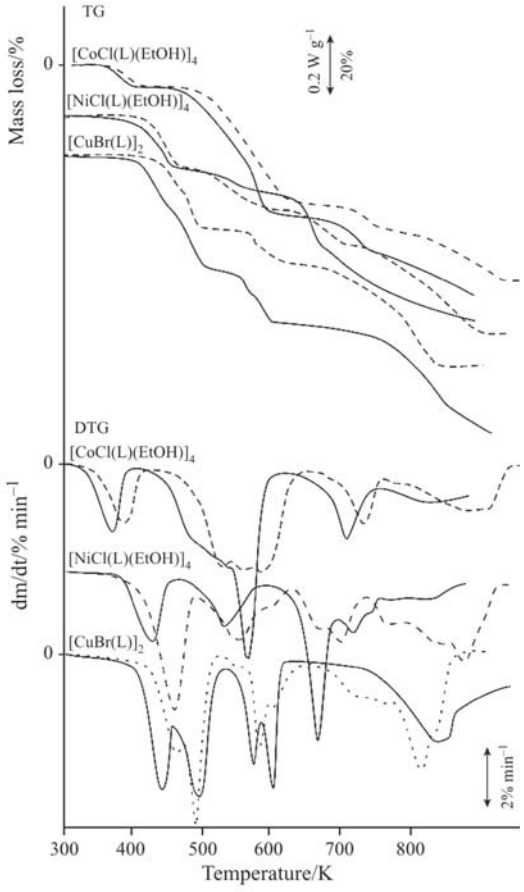

Fig. 3 TG-DTG curves of complexes with HL, — – in argon, - - - – in air

Table 4 M–O(EtOH) distances in (**V**) and (**VI**) in Å*

Co(1)–O(16)	2.135(2)	Ni(1)–O(9)	2.062(3)
Co(2)–O(13)	2.1420(19)	Ni(2)–O(13)	2.070(3)
Co(3)–O(14)	2.1493(19)	Ni(3)–O(15)	2.084(3)
Co(4)–O(10)	2.108(2)	Ni(4)–O(20)	2.084(3)
$l_{(Co-O)(average)}$	2.133 Å	$l_{(Ni-O)(average)}$	2.075 Å
Δ_{max}	0.041 Å	Δ_{max}	0.022 Å

*The Ni–O(EtOH) distances are determined under the same conditions as the corresponding Co–O(EtOH) distances. (ΔrCo(II)–Ni(II))=0.03 Å, [43])

pare the corresponding distances and the thermal decomposition pattern for more isostructural solvates. In addition, the thermal decomposition depends on many, hardly controllable experimental conditions, among others on the porosity of the samples, particle sizes, etc. In order to check the reproducibility of the TG measurement, the TG runs for these two samples were repeated six times. The decomposition, within the experimental uncertainty, was the same in all measurements. However, to support the above proposition, further coupled crystal structural and thermal experimental data are needed.

The thermal decomposition of **IV**, $[CuBr(L)]_2$, shows a different course. In the absence of solvate molecules the decomposition temperature is somewhat higher (420 K) compared with that of **V** and **VI**. In contrast to the usual thermal behavior of similar complexes where the decomposition pattern in argon does not depend on the atmosphere up to about 600 K and above this temperature the decomposition slows down, the TG curves of **IV** suggest a different decomposition

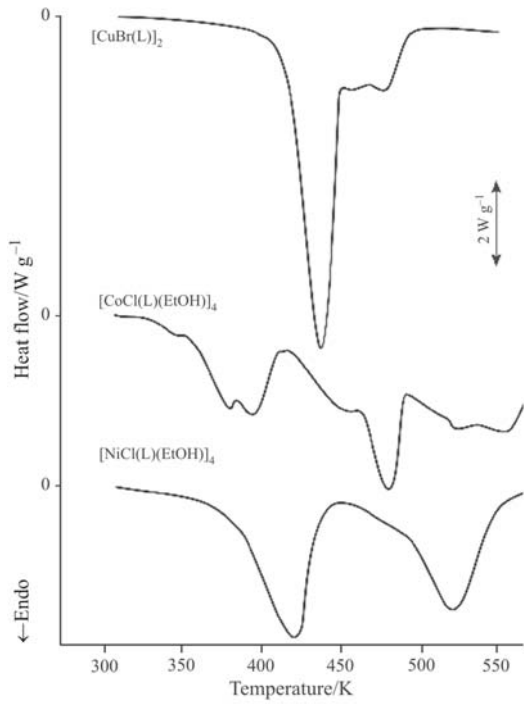

Fig. 4 DSC curves of the complexes with HL

mechanism in different atmospheres. In argon the superimposing decomposition steps are better separated. At about 650 K the DTG falls almost to zero and the mass loss agrees to the formation of CuBr per monomer unit (found, 45.2%; calcd: 46.59%). However, in lack of TG-MS coupled measurement, this conclusion is only optional. The decomposition is completed with some coke residue around 1000 K. In air the end product at 850 K is CuO (found: 30.6%, calcd: 29.61%).

The corresponding DSC curves (Fig. 4) show endothermic decomposition for all three compounds. Due to the beginning of the decomposition, the shape of the curves does not refer to melting of the compounds which was visually observed in the case of **IV** and **V**. Complexes **VI** and **III** appear in form of greyish green and black powder, respectively, after desolvation. The evaporation steps of the first two EtOH molecules in **V** complex are clearly separated in the DSC diagram in accordance with the corresponding DTG curve.

Conclusions

$CuCl_2$ forms two *dmp* complexes with HL as a consequence of the splitting of the 1-N-hydroxymethyl group. In the case of $CuBr_2$, $NiCl_2$ and $CoCl_2$ the complex formation was studied in the presence of base (KOH) and without it. It was found that the ligand deprotonation is spontaneous with $NiCl_2$. In the reaction with $CoCl_2$ in basic solution two products were obtained in the form of single crystals: $CoCl_2(dmp)_2$ is the primary product both at room temperature and under reflux. The crystallization of $[CoCl(EtOH)]_4$ takes place from the mother liquid in deep freezer. When the reaction is carried out with cold solutions, in deep freezer, the only product is $[CoCl(EtOH)]_4$ with low yield. The crystal structure of this complex was determined by X-ray diffraction. $[CuBr(L)]_2$ was obtained from basic solution with a 1:2 metal-to-ligand ratio. Its structure was proposed on the basis of elemental analysis data and IR spectral analysis. The thermal decomposition of the compounds is continuous. The different desolvation pattern of the isomorphous $[MCl(EtOH)]_4$ complexes is most probably the consequence of different complex formation preference of $CoCl_2$ with HL. The decomposition of all discussed complexes is endothermic in the whole investigated temperature range, accompanied with the melting of **IV** and **V**.

Supplementary material

A full list of crystal data and refinement of **V** has been deposited at the Cambridge Crystallographic Data Centre, CCDC No. 604068.

Acknowledgements

The work was financed in part by the Ministry for Science and Environmental Protection of the Republic of Serbia (Grant N^{o} 142028) and Provincial Secretariat for Science and Technological Development of Vojvodina. Additional financial support from the Hungarian Scientific Research Foundation (OTKA No. T038189) and computational time from the National Information Infrastructure Development Program of Hungary is gratefully acknowledged. M. Sz. K. thanks the Arany János and A. K. the Bolyai Foundation for support. The authors would like to thank Ivana Radosavljević Evans (Dept. of Chemistry, University of Durham) for solving the crystal structure of **V**.

References

1 R. C. Elderfield, (Ed.), Heterocyclic Compounds, John Wiley, New York 1959, p. 565.
2 W. G. Haanstra, Ph.D. Thesis, Leiden University, 2300 RA Leiden, The Netherlands 1991.
3 W. G. Haanstra, W. A. J. W. van der Donk, W. L. Dreissen, J. Reedijk, J. S. Wood and M. G. B. Drew, J. Chem. Soc. Dalton, (1990) 3123.
4 E. I. Solomon, U. M. Sundaram and T. E. Machonkin, Chem. Rev., 96 (1996) 2563.
5 R. Mukherjee, Coord. Chem. Rev., 203 (2000) 151.
6 P. Gamez, J. von Harras, O. Roubeau, W. L. Driessen and J. Reedijk, Inorg. Chim. Acta, 324 (2001) 27.
7 J. E. Cosgriff and G. B. Deacon, Angew. Chem., Int. Ed. Engl., 37 (1998) 286.
8 E. C. Plappert, T. Stumm, H. van der Bergh, R. Hauert and K.-H. Dahmen, Chem. Vap. Deposition, 3 (1997) 37.
9 C. Pettinari, F. Marchetti, C. Santini, R. Pettinari, A. Drozdov, S. Troyanov, G. A. Battiston and R. Gerbasi, Inorg. Chim. Acta, 315 (2001) 88.
10 M. Krunks, J. Madarász, T. Leskelä, A. Mere, L. Niinistö and G. Pokol, J. Therm. Anal. Cal., 72 (2003) 497.
11 R. Mrozek-Łyszczek, J. Therm. Anal. Cal., 78 (2004) 473.
12 J. Madarász, M. Krunks, L. Niinistö and G. Pokol, J. Therm. Anal. Cal., 78 (2004) 679.
13 I. Labádi, Zs. Czibulya, R. Tudose, O. Costisor and R. Mrozek-Łyszczek, J. Therm. Anal. Cal., 78 (2004) 965.
14 D. Czakis-Sulikowska, J. Radwańska-Doczekalska, A. Czylkowska and J. Gołuchowska, J. Therm. Anal. Cal., 78 (2004) 501.
15 C. Bâtiu, I. Panea, L. Ghizdavu, L. David and S. Ghizdavu Pellascio, J. Therm. Anal. Cal., 79 (2005) 129.
16 T. Premkumar and S. Govindarajan, J. Therm. Anal. Cal., 79 (2005) 115.
17 K. Mészáros Szécsényi, V. M. Leovac, Ž. K. Jaćimović, V. I. Češljević, A. Kovács, G. Pokol and S. Gál, J. Therm. Anal. Cal., 63 (2001) 723.
18 K. Mészáros Szécsényi, V. M. Leovac, Ž. K. Jaćimović, V. I. Češljević, A. Kovács and G. Pokol, J. Therm. Anal. Cal., 66 (2001) 573.
19 K. Mészáros Szécsényi, V. M. Leovac, V. I. Češljević, A. Kovács, G. Pokol, Gy. Argay, A. Kálmán, G. A. Bogdanović, Ž. K. Jaćimović and A. Spasojević-de Biré, Inorg. Chim. Acta, 353 (2003) 251.
20 K. Howard, I. R. Evans, K. Mészáros Szécsényi, V. M. Leovac and Ž. K. Jaćimović, J. Coord. Chem., 57 (2004) 469.
21 A. Kovács, D. Nemcsok, G. Pokol, K. Mészáros Szécsényi, V. M. Leovac, Ž. K. Jaćimović, I. R. Evans, J. A. K. Howard, Z. D. Tomić and G. Giester, New J. Chem., 29 (2005) 833.
22 S. Trofimenko, Chem. Rev., 72 (1972) 447.
23 S. Trofimenko in S. J. Lippard (Ed.), Progr. Inorg. Chem., Wiley New York, 34 (1986) 115–210.
24 S. Trofimenko, Chem. Rev., 93 (1993) 943.
25 V. Chandrasekhar, S. Kingsley, A. Vij, K. C. Lam and A. L. Rheingold, Inorg. Chem., 39 (2000) 3238.
26 R. Oki, J. Sanchez, S. Hamilton and T. J. Emge, J. Coord. Chem., 36 (1995) 63.
27 F. Paap, E. Bouwman, W. L. Driessen, R. A. G. de Graaff and J. Reedijk, J. Chem. Soc. Dalton Trans., (1985) 737.
28 G. M. Sheldrick, SADABS, University of Göttingen, Germany 1998.
29 SAINT+, Release 6.22. Bruker Analytical Systems, Madison, Wisconsin, USA 1997–2001.
30 G. Altomare, G. Cascarano, A. Giacovazzo, M. C. Guagliardi, G. Burla, G. Polidori and M. Camalli, J. Appl. Crystallogr., 27 (1994) 435.
31 P. W. Betteridge, J. R. Carruthers, R. I. Cooper, K. Prout and D. J. Watkin, J. Appl. Crystallogr., 36 (2003) 1487.
32 B. Barszcz, T. Glowiak, J. Jezierska and K. Kurdziel, Inorg. Chem. Commun., 5 (2002) 1056.
33 B. Barszcz, T. Glowiak, J. Jezierska and A. Tomkiewicz, Polyhedron, 23 (2004) 1309.
34 R. G. Pearson, J. Am. Chem. Soc., 85 (1963) 3533.
35 R. G. Pearson and J. Songstad, J. Am. Chem. Soc., 89 (1967) 1827.
36 T.-L. Ho, Chem. Rev., 75 (1975) 1.
37 S. Tanase, E. Bouwman, W. L. Driessen, J. Reedijk and R. de Gelder, Inorg. Chim. Acta, 355 (2003) 458.
38 I. R. Evans, J. A. K. Howard, L. E. M. Howard, J. S. O. Evans, Ž. K. Jaćimović, V. S. Jevtović and V. M. Leovac, Inorg. Chim. Acta, 357 (2004) 4528.
39 P. J. Hay and W. R. Wadt, J. Chem. Phys., 82 (1985) 270.
40 K. Nakamoto, Infrared and Raman Spectra of Inorganic and Co-ordination Compounds. Part B. Applications in Co-ordination, Organometallic and Bioinorganic Chemistry, Wiley, New York 1997, 5th Ed.
41 B. Neinding, Magnetochemistry of Transition Metal Complexes, Results in Sciences (Series Chemistry), Moscow 1970, p. 205 (in Russian).
42 H. Remy, Lehrbuch der Anorganischen Chemie, Akad. Verlagsgesellschaft, Leipzig 1950.
43 V. I. Dulova, A. P. Myagchenco, V. D. Kolotyk and K. K. Yu. Chotii, Koord. Khim., 8 (1982) 1103.
44 R. D. Shannon, Acta Cryst., A32 (1976) 751.

Received: March 3, 2006
Accepted: April 12, 2006
OnlineFirst: August 11, 2006

DOI: 10.1007/s10973-006-7564-8